



HAL
open science

Effect of carbon dioxide on self-setting apatite cement formation from tetracalcium phosphate and dicalcium phosphate dihydrate; ATR-IR and chemoinformatics analysis

Yuta Otsuka, Masaki Takeuchi, Makoto Otsuka, Besim Ben-Nissan, David Grossin, Hideji Tanaka

► To cite this version:

Yuta Otsuka, Masaki Takeuchi, Makoto Otsuka, Besim Ben-Nissan, David Grossin, et al.. Effect of carbon dioxide on self-setting apatite cement formation from tetracalcium phosphate and dicalcium phosphate dihydrate; ATR-IR and chemoinformatics analysis. *Colloid and Polymer Science*, 2015, 293 (10), pp.2781-2788. 10.1007/s00396-015-3616-6 . hal-01490595

HAL Id: hal-01490595

<https://hal.science/hal-01490595>

Submitted on 15 Mar 2017

HAL is a multi-disciplinary open access archive for the deposit and dissemination of scientific research documents, whether they are published or not. The documents may come from teaching and research institutions in France or abroad, or from public or private research centers.

L'archive ouverte pluridisciplinaire **HAL**, est destinée au dépôt et à la diffusion de documents scientifiques de niveau recherche, publiés ou non, émanant des établissements d'enseignement et de recherche français ou étrangers, des laboratoires publics ou privés.



Open Archive Toulouse Archive Ouverte (OATAO)

OATAO is an open access repository that collects the work of Toulouse researchers and makes it freely available over the web where possible.

This is an author-deposited version published in: <http://oatao.univ-toulouse.fr/>
Eprints ID: 16543

To link to this article: DOI: [10.1007/s00396-015-3616-6](https://doi.org/10.1007/s00396-015-3616-6)
<http://dx.doi.org/10.1007/s00396-015-3616-6>

To cite this version:

Otsuka, Yuta and Takeuchi, Masaki and Otsuka, Makoto and Ben-Nissan, Besim and Grossin, David and Tanaka, Hideji *Effect of carbon dioxide on self-setting apatite cement formation from tetracalcium phosphate and dicalcium phosphate dihydrate; ATR-IR and chemoinformatics analysis*. (2015) Colloid and Polymer Science, vol. 293 (n° 10). pp. 2781-2788.
ISSN [0303-402X](https://doi.org/10.1007/s00396-015-3616-6)

Any correspondence concerning this service should be sent to the repository administrator: staff-oatao@listes-diff.inp-toulouse.fr

Effect of carbon dioxide on self-setting apatite cement formation from tetracalcium phosphate and dicalcium phosphate dihydrate; ATR-IR and chemoinformatics analysis

Yuta Otsuka¹ · Masaki Takeuchi² · Makoto Otsuka³ ·
Besim Ben-Nissan⁴ · David Grossin⁵ · Hideji Tanaka²

Abstract Rapid self-setting apatite cement (SSAC) formation from tetracalcium phosphate (TeCP) and dicalcium phosphate dihydrate (DCPD) has been investigated by an attenuated total reflection Fourier transform infrared (ATR-IR) spectroscopy coupled with a principal component analysis (PCA). After TeCP and DCPD were kneaded with phosphoric acid, the peaks of ATR-IR spectra for the kneaded sample shift significantly in the ranges of 2250-2400 and 850-1150 cm⁻¹ due to the crystalline transformation into hydroxyapatite (HAp). The PCA results indicate that the loadings of principal components 1 and 2 (PC1 and PC2, respectively) are ascribed to CO₂ and phosphate group, respectively, in the transforming cement. The PC1 score initially increases to reach a maximum at around 1000 s and then decreases. In contrast, the PC2 score increases continuously, but its increment became lesser with time. Although the profiles of PC2 score against PC1 score are similar in shape, there are deviations among the profiles obtained through quadruplicate

experiments. The scores are, therefore, time differentiated, and the relationship between the differentiated scores is analyzed. The time differentiation approach is found to be useful for understanding complicated chemical reactions. The PCA results suggest that SSAC formation can be divided into three major stages. In the first stage, CO₂ concentration in the transforming cement rapidly increases, which triggers HAp crystallization. In the second stage, CO₂ concentration still increases, but its increasing rate drastically decreases; HAp crystallization continues with increasing rate. In the last stage, CO₂ concentration decreases, and HAp crystallization significantly slows down.

Keywords Self-setting apatite cement · Hydroxyapatite · Attenuated total reflection Fourier transform infrared spectroscopy · Principal component analysis · Crystalline transformation · Differentiated scores

Yuta Otsuka
y.otsuka36156803@gmail.com

¹ - Graduate School of Pharmaceutical Sciences, Tokushima University, 1-78-1 Shomachi, Tokushima 770-8505, Japan

² Institute of Health Biosciences, Tokushima University, 1-78-1 Shomachi, Tokushima 770-8505, Japan

³ Research Institute of Pharmaceutical Sciences, Faculty of Pharmacy, Musashino University, 1-1-20 Shinmachi, Nishi-Tokyo 202-8585, Japan

⁴ Faculty of Science, School of Chemistry and Forensic Science, University of Technology Sydney, Sydney, NSW, Australia

⁵ CIRIMAT Carnot Institute, University of Toulouse, INPT-UPS-CNRS UMR 5085, Toulouse, France

Introduction

Hydroxyapatite (Ca₁₀(PO₄)₆(OH)₂; HAp) (more strictly, non-stoichiometric substituted HAp) is a major constituent of bone (60 % by weight) and has high biocompatibility. In the field of biomaterials, bioactive HAp bone cements are generally produced from tetracalcium phosphate (Ca₄(PO₄)₂; TeCP) and dicalcium phosphate dihydrate (CaHPO₄ · 2H₂O; DCPD) in the presence of phosphoric acid. This kind of bone cement, which contains remaining TeCP and DCPD, is called "self-setting apatite cement (SSAC)." The cement has moderate crystallinity with similar characteristics to mammalian bone [1-3] and high biocompatibility. It is often used as a bone filler for bone defects in orthopaedic surgery [4]. Hamanishi et al. reported a new drug delivery system

(DDS) for vancomycin, based on SSAC; the DDS-SSAC was successfully applied to the treatment of methicillin-resistant *Staphylococcus aureus* osteomyelitis [5]. Hamada et al. reported a DDS-SSAC containing simvastatin, and the medium-responsive release of the drug in vitro. They investigated bone mineral density change after the implantation of the DDS-SSAC in osteoporotic rats by means of an X-ray computed tomography [6].

Miyamoto et al. quantitatively measured the transformation of TeCP and dicalcium phosphate anhydrate (DCPA) into HAp by a powder X-ray diffraction analysis (XRD) [7]. XRD is, however, not sufficient to measure the self-setting process, because XRD cannot follow rapid reaction in minutes or shorter. In addition, the method requires relatively large amount of samples (>0.1 g). It is, therefore, highly desirable to clarify the self-setting mechanism of HAp from TeCP, DCPD (or DCPA) in order to develop new generation biomaterials.

Fourier transform infrared (FT-IR) spectroscopy is one of the most versatile analytical methods for the identification of materials and the quantification of their components. The spectroscopy can afford chemical and/or physical information on the materials with IR-active vibrations (symmetrical/anti-symmetrical stretching, scissoring, etc.), light diffusivity, and so on. The relationship between IR absorbance and the concentration of the component obeys Lambert-Beer's law. Petrov and Soptrajanov successfully applied FT-IR spectroscopy to the characterization of metastable calcium phosphates [8]. Changa et al. [9] employed FT-IR spectroscopy to analyze the cross-linking of the HAp/Collagen nano-composite. Conventional FT-IR spectroscopy requires, however, sample dilution with potassium bromide powder, because its sensitivity is too high to measure raw materials. Attenuated total reflection (ATR)-IR spectroscopy can overcome such shortcomings of FT-IR spectroscopy and rapidly measure a few milligrams of sample in monolithic, thin film-like or liquid form without dilution [10, 11].

Chemoinformatics is a combination of mathematical and statistical methods for the design or selection of the optimal conditions of experiments and for the derivation of utmost pieces of chemical information through the analysis of acquired data [12, 13]. Principal component analysis (PCA) is a multivariate analysis that can be used for the analyses of reaction kinetics and of spectra obtained by spectroscopies [14].

We have been studying on the polymorphic transition of drugs in pharmaceutical tablet by means of XRD [15] or FT-near infrared spectroscopy coupled with Chemoinformatics [16]. In the present study, we propose an ATR-IR- and PCA-based approach for the elucidation of the reaction mechanism of rapid self-setting apatite formation from TeCP-DCPD suspension.

Materials and methods

Materials

TeCP and DCPD powders were purchased from Taihei Chemical Industrial Co. (Osaka, Japan) and Wako Pure Chemical Industries (Osaka, Japan), respectively. The apatite cement was prepared according to the procedure described by Brown and Chow [1]. The raw material for the preparation of the cement powder was an equimolar mixture of TeCP and DCPD powders, in which the molar ratio of Ca/P was 1.67.

Powder X-ray diffraction analysis

The raw material, which had been stored at high humidity, was carefully ground in an agate mortar with a pestle. Loosely packed sample was prepared in order to avoid crystal orientation when it was poured in the holder of the instrument without compression. The crystal phases in the specimens thus prepared were analyzed with a powder X-ray diffraction (XRD) system (Miniflex, Rigaku Co., Ltd., Tokyo, Japan) at room temperature. Measurement conditions were as follows: Ni-filtered CuK α radiation ($\lambda=0.1540$ nm); voltage, 30 kV; current, 15 mA; time constant, 1 s; step slit, 0.2°; counting time, 1.0 s; and measurement range, 2 θ =5.0-45.0°.

Infrared spectroscopy measurement

Infrared spectra were measured with an FT-IR spectrometer (FT/IR-6500, JASCO Co., Tokyo, Japan) equipped with an ATR accessory, which was inserted directly in the light beam. Five milligrams of mixed TeCP-DCPD powder was kneaded with 20.0 μ L of 11.0 mmol/L phosphoric acid. The paste was put on a germanium glass of the ATR accessory and covered with a sheet of Parafilm® at room temperature. IR spectra of the suspensions were measured in the range of 600-3800 cm^{-1} at a resolution of 8 cm^{-1} and acquired as digital data in a computer for further kinetic analysis. The data of 120 scans were normalized based on the area under the observed spectrum [17] and corrected, where air spectrum was subtracted from the averaged spectrum as a background.

Software

The chemoinformatics calculations were performed by UNSC RAMBLER software version 10.2 from CAMO (Computer Aided Modelling, Trondheim, Norway).

Principal component analysis

Although ATR-IR spectra can be represented in n-dimensional space, it is difficult to comprehend the data in the dimensions more than three. It is, therefore, useful to reduce the

dimensionality of the multidimensional spectral space [18]. Multivariate analysis methods such as PCA can reduce the dimensionality of multidimensional space while retaining most of the original information in the data set. PCA operates by obtaining eigenvalues of the variance-covariance matrix (S) of the origin of data set and the eigenvectors. Calculation of the eigenvalues and eigenvectors can be accomplished readily via the singular value decomposition of S . The mean centered data matrix X is, therefore, reduced to the sum of a cross-product of two smaller matrixes, P and T , and a residual matrix, E ,

$$X = TPT + E \quad (1)$$

where T is the matrix of the eigenvectors (loadings) and P is the matrix of scores. The cross-product of TPT contains most of the original variance in X . This term (TPT) is the structured part of the data: the part that is most informative. The remain (E) represents the fraction of variation that cannot be modelled well [17].

Results and discussion

XRD analysis

Figure 1 shows the powder X-ray diffractograms of SSAC, TeCP, equimolar mixture of DCPD and TeCP raw cement, and DCPD; SSAC was prepared through kneading the TeCP-DCPD mixture (5.0 g) with 11.0 mmol/L phosphoric acid (20.0 μ L) for 1 day. The profile of SSAC shows broad peaks at 25.8°, 31.6°, and 32.7° that are characteristic of HAp. The profile of TeCP has distinct peaks at 25.2°, 27.8°, 28.1°, 29.1°, 29.6°, 31.0°, 32.1°, 33.8°, 35.3°, 36.1°, 38.6°, and 40.8°. That of DCPD does so at 11.5°, 20.8°, 23.3°, 29.2°, 30.4°, 34.0°,

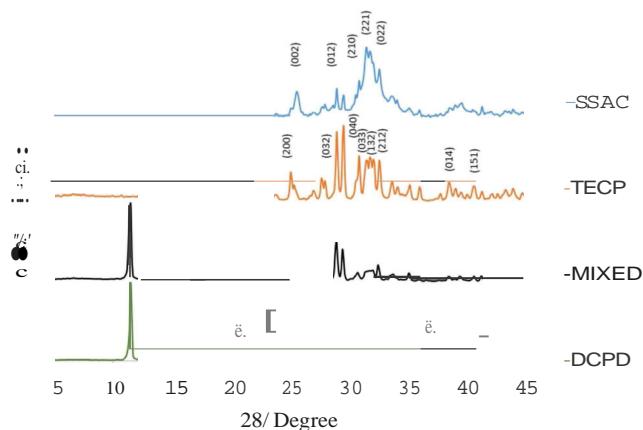


Fig. 1 XRD profiles of apatite cement before and after setting. *MIXED* equimolar mixture of TeCP and DCPD before the setting, *SSAC* self-setting apatite cement prepared through the kneading of *MIXED* (5 g) with 20.0 μ L of 11.0 mmol/L phosphoric acid for 1 day

39.6°, and 41.5°. These results indicate that the bulk powder of TeCP-DCPD mixture transforms into HAp, but very small amounts of DCPD (28=29.2°) and TeCP (28=25.2°) are remained. Similar results were reported by Hayakawa et al. [19, 20].

ATR-IR spectroscopy

Figure 2 shows the temporal change of corrected ATR-IR absorption spectra of the TeCP-DCPD mixture kneaded with phosphoric acid. The peaks in the ranges of 1500-1700 and of 2800-3800 cm^{-1} are due to free water in aqueous phase. The spectra show characteristic peak shifts in the ranges of 2250-2400 and 850-1150 cm^{-1} , attributable to the formation of HAp. As for the latter range, it is known that the absorption bands of HAp-related materials are, respectively, assigned to as follows [21-23]: the band at 3569 cm^{-1} to hydroxyl stretch and the bands at 962, 472, 976-1190, and 520-660 cm^{-1} to ν_1 , ν_2 , ν_3 , and ν_4 vibrational modes of phosphate ions, respectively. At 5400 s after the kneading, the IR spectra of SSAC showed more characteristic peaks in the range of 850-1150 cm^{-1} , compared to at 0 s, due to phosphate ions.

The CO_3 ν_3 broad peaks could faintly be seen in 1400-1550 cm^{-1} in this figure. It is known that CO_3 is contained in HAp products as an impurity. Such carbonated HAp is generally classified as A-type or B-type [24, 25]. Carbonate ion is substituted with OH (type A) or PO_4 (type B) in HAp. Type A carbonate gives doublet bands at about 1545 and 1450 cm^{-1} (asymmetric stretching vibration, ν_3) and 880 cm^{-1} (out-of-plane bending vibration, ν_2); type B carbonate gives three bands at about 1455, 1410, and 875 cm^{-1} [26, 27]. The CO_3 ν_2 peaks could be seen faintly at 871 cm^{-1} in this figure. This result suggests that B-type carbonate HAp is produced in the present study.

Figure 3 shows the normalized ATR-IR spectra in the ranges of 2250-2400 and 850-1150 cm^{-1} . The spectral

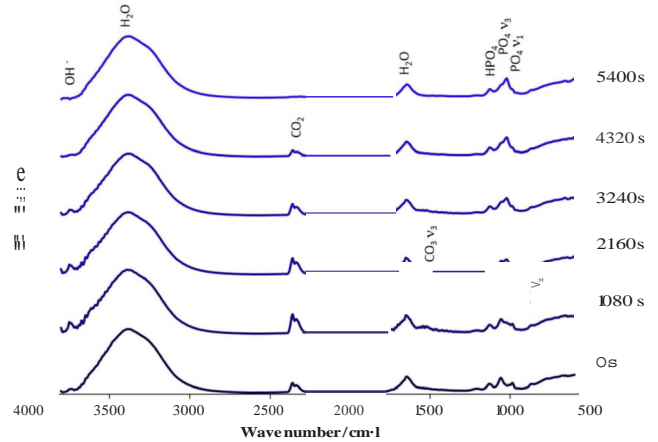
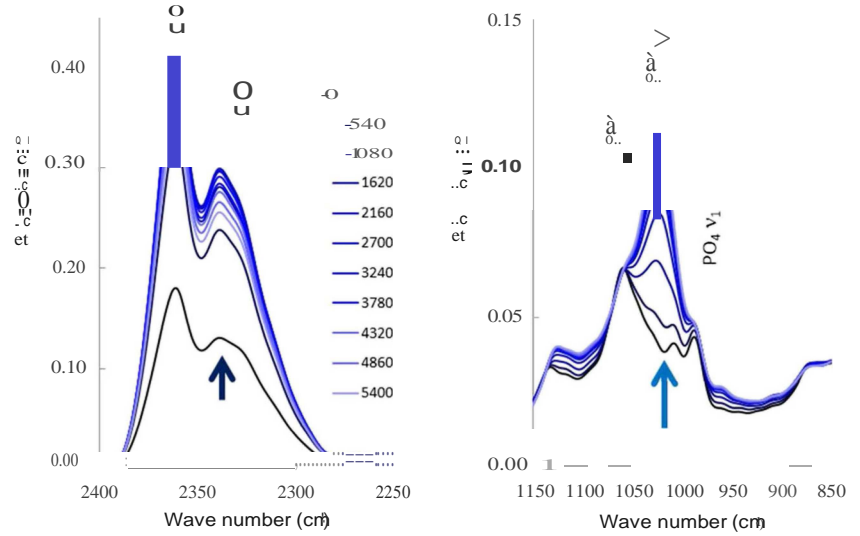


Fig. 2 Temporal profiles of ATR-IR spectra of apatite cement in the course of the setting

Fig. 3 The normalized ATR-IR spectra in the ranges of 850-1150 and 2250-2500 cm^{-1}



change suggests that TeCP and DCPD in the raw cement have transformed into HAp by the kneading. That is, the absorption peak by phosphate group shifts from 1058 cm^{-1} (HPO_4) to 1024 cm^{-1} (PO_4), indicating the crystal transition to HAp from the raw cement [28]. The peaks at 2360 and 2340 cm^{-1} due to CO_2 did not shift, but their intensities changed in a complex manner in the course of the formation of HAp. This result will be discussed in later section.

Principal component analysis

The normalized absorbance in the ranges of $850\text{--}1150$ and $2250\text{--}2400 \text{ cm}^{-1}$ (Fig. 3), which, respectively, correspond to CO_2 and phosphate group, is analyzed by PCA. In the present PCA computation, ATR-IR absorbance at each wavenumber is regarded as the variable. Total residual variances for PCA, which was based on the change of ATR-IR spectra during the cement setting, were 4.14 and 1.20 % for PC1 and PC2,

respectively. It is important to control the number of principal component (PC) in multivariate analysis such as PCA, because unsuitable number of PC may cause unclear results. In order to clarify HAp formation, the effect of PC number of explain parameters should also be examined in detail. Ideally, simple models with minimal components, where the residual variance is ultimately zero, should be searched. The smaller total residual variance is, the more pieces of information in the variation can be explained. If this is not the case, it means that there are considerable noises in the data and/or that the data structure is too complex to be accounted for with a small number of components [17]. The residual variance of multivariate analysis of ATR-IR spectra has not only a quantitative analytical result but also qualitative chemical information about the products. As described in the previous section, the normalized ATR-IR spectra have information regarding to CO_2 in the suspension and phosphate group in HAp. Number of PCs for PCA needs, therefore, to be at least two so as to

Fig. 4 Loading vectors PC1 (left) and PC2 (right) for PCA

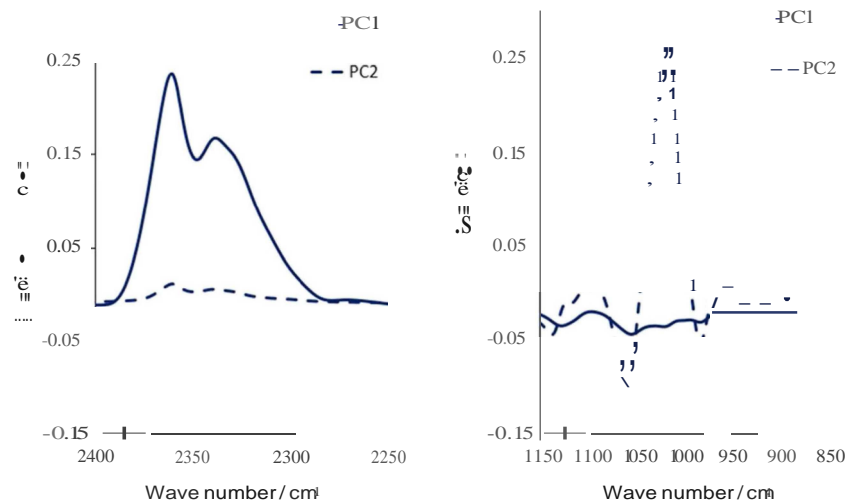
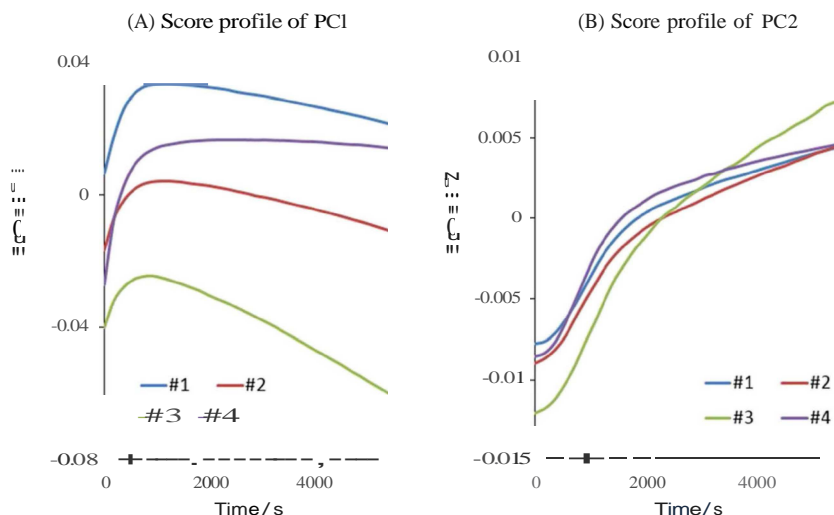


Fig. 5 Score profiles of PC1 (a) and PC2 (b) for the ATR-IR spectral data matrix of each SSAC setting process



explain the change of ATR-IR spectra in the course of self-setting HAp formation.

Figure 4 shows the loadings of PC1 and PC2 for PCA in the ranges of 850-1150 and 2250-2500 cm^{-1} . PC1 has significant peaks in the range of 2250-2400 cm^{-1} , but does not have in the range of 850-1150 cm^{-1} . In contrast, PC2 has such peak in the range of 850-1150 cm^{-1} , but does not have in the range of 2250-2400 cm^{-1} . These results indicate that PC1 and PC2, respectively, correspond to CO_2 and phosphate group.

Figure 5a, b shows the score profiles of PC1 and PC2 in the ATR-TR spectral data matrix of each SSAC sample as a function of setting time. Since the spectra are absorption profiles following Lambert-Beer's law, the obtained scores of PC1 and PC2 correspond to the concentrations of CO_2 and phosphate group, respectively. The score profiles of PC1 (A) increased initially, reached to a maximum at around 1000 s, and then decreased. Although the variation of the scores is large between the samples, the tendencies are similar among them. In contrast, the score of PC2 (B) increased sigmoidally.

Figure 6 shows the relationships between the scores of PC1 and PC2 for the samples. Initially, the change of PC1 is more significant than that of PC2. All profiles are similar in shape, but the variation in their values, especially in those of PC1, are very large. The baseline shift in ATR-IR spectra, resulted from the differences in powder density, size distribution, and background humidity are considered to attribute to the variation.

PCA with score differentiate analysis

In order to eliminate the variations among samples, the scores were differentiated with respect to time. The information regarding to time are not reduced and still contained in the scores and their differential values. Figure 7a, b shows thus obtained differential scores of PC1 and PC2, respectively. The time-differentiated PC1 scores increased initially with time, reached maxima at 180 s, and then decreased to zero at around 1000 s.

Fig. 6 Relationship between PC1 and PC2 scores for each SSAC setting process. Arrow indicates the time course of the process

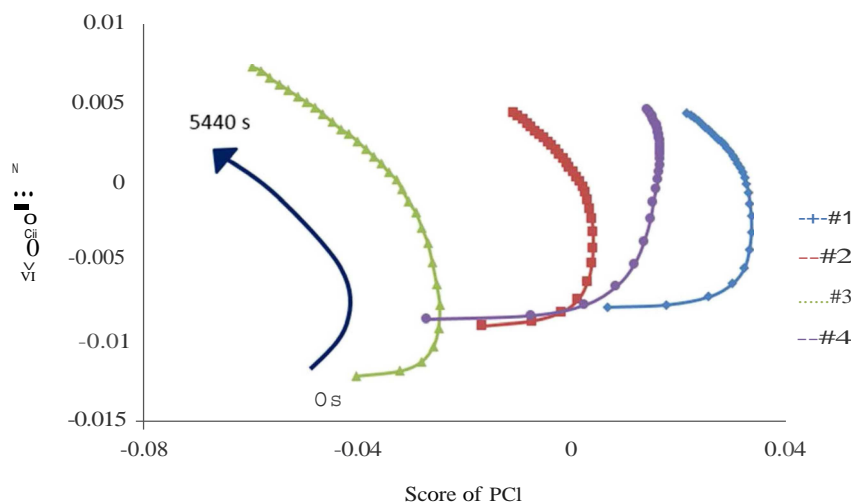
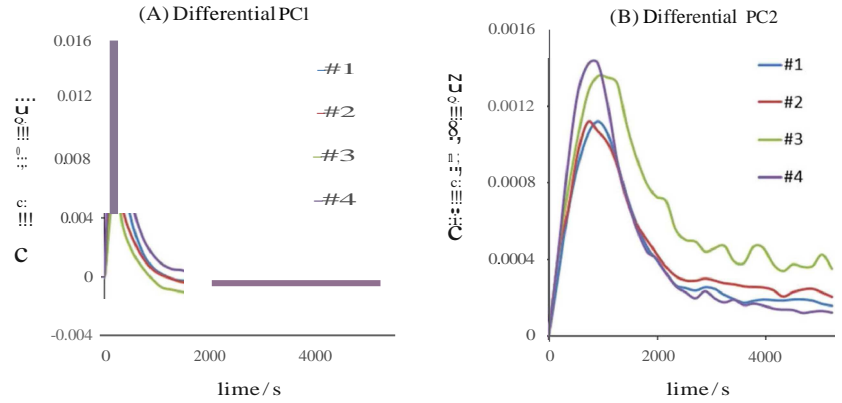


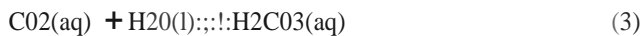
Fig. 7 Differentiated PC1(a) and PC2 (b) score profiles for each SSAC phase transformation process



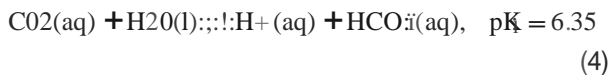
After 2000 s, the scores become almost constant and have negative values. In contrast, the differentiated PC2 scores increased slowly, reached to maxima around 1000 s in contrast with 180 s for differentiated PC 1, and then decreased.

Figure 8 shows the relationship between differentiated scores of PC1 and PC2. It suggests that the transformation of SSAC consists of three major stages. In the first stage, the concentration change rate of CO₂ (corresponding to PC1) rapidly increases, and the recrystallization relating to phosphate group vibration (corresponding to PC2) starts. In the second stage, the concentration change rate of CO₂ decreases with time, but the crystallization rate still increases constantly. In the last stage, the concentration change rate of CO₂ slightly decreases to a negative value, and the HAp crystallization rate significantly decreases. From these results, CO₂ is considered to be not only the source of CO₃²⁻ of carbonated HAp but also a catalyst for HAp formation. Referring to the report by Welch et al. [29], chemical reaction between the calcium phosphates and CO₂ is considered to be expressed as follows:

Henry's law indicates that the partial pressure of CO₂ gas is proportional to CO₂ concentration in suspension (Eqs. 2 and 3). CO₂ concentration in atmospheric air is constant at 381 ppmv (=5.5 v/v%).

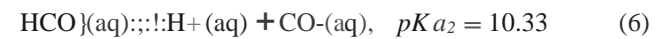


The hydration constant K_h for the reaction of Eq. 3 is $1.7 \times 10^{-3} \text{ mol/L}$ at 25 °C.



$$K_{a1}^* = \frac{[\text{H}^+][\text{HCO}_3^-]}{[\text{H}_2\text{CO}_3] + [\text{CO}_2]} = 4.45 \times 10^{-7} \text{ mol/L} \quad (5)$$

where K_{a1} means the apparent first dissociation constant of carbonate acid, taking CO₂ concentration into account.



$$K_{a2} = \frac{[\text{H}^+][\text{CO}_3^{2-}]}{[\text{HCO}_3^-]} = 4.7 \times 10^{-11} \text{ mol/L} \quad (7)$$

CO₂ is ionized to CO₃²⁻ (Eqs. 3, 4, 6), the concentration of which is expressed in Eq. 7.

The reactions of Eqs. 2-4 and 6 are reversible.

Fukase et al. [30] reported that the raw TeCP-DCPD cement transformed into stoichiometric HAp as follows:

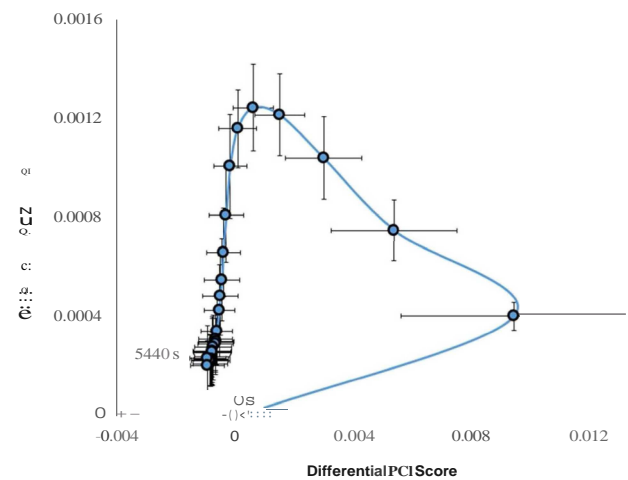
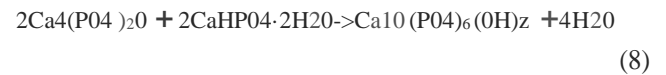
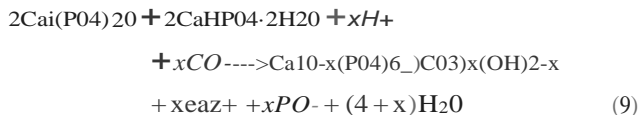


Fig. 8 Relationship between differentiated PC1 and PC2 scores for SSAC setting process. Horizontal and vertical bars indicate respective standard deviation (n=4)

Otsuka et al. [31] elucidated through their study employing FT-IR spectroscopy that an apatite cement transformed into carbonated HAp while absorbing a small amount of carbonate ion; carbonate ion in the carbonated HAp could be removed by laser irradiation. Hsu et al. reported that the chemical formulation of B-type carbonated HAp in mammalian bone was $[\text{Ca}_{10-x}\text{Na}_x(\text{PO}_4)_6-x(\text{CO}_3)_x(\text{OH})_2]$ [19]. The present results indicate that the bulk powders of TeCP and DCPD irreversibly transformed into carbonated HAp in the presence of CO_2 after its being mixed with a kneading solution (Eq. 9).



From Eq. 9, the pH of the solution is considered to increase during the transformation. Doi et al. reported that the pH of the suspension changed from acidic to natural when TeCP and DCPD dissolved in 20 mM phosphoric acid at the powder/liquid ratio of 5 mL/g [32].

In the first stage of phase transition, CO_2 concentration (PCI) in the suspension increased (see Figs. 5 and 6). Both CO_2 in the solution and that on the solid surface contribute to the CO_2 concentration measured by ATR-IR. The CO_2 concentration in the solution is constant because the atmospheric CO_2 concentration is virtually invariable (Eq. 2). The present results suggest, therefore, the absorption/adsorption of CO_2 in/on the transformed solid from CO-rich supersaturated calcium phosphate solution, presumably, at the initial stage of transformation. In the second stage, the supersaturated solution formation still continued but some of them transformed to carbonated HAp while releasing excess CO_2 . This release results in the decrease of differential score of PCI (Figs. 7 and 8). In the last stage, the reaction is approaching to the completion which means carbonated HAp formation, resulting in the negative differential score of PCI. The CO_2 acts, therefore, as a catalyst or mediator for the phase transition in addition to the source of carbonate ion in carbonated HAp. Although the final composition of the solid phase is not completely clear in the present study because the transformation was measured for 5400 s, some CO_2 molecules may be remained in the final product (carbonated HAp) without being converted to carbonate ion. Welch et al. reported such phenomena before [29]. Eidelman et al. measured the solubility of various types of calcium phosphates in the presence and absence of 5.5 % CO_2 in the atmosphere. At 5.5 % CO_2 concentration, undiluted ultrafiltered human serum was substantially under saturated, slightly supersaturated, and highly supersaturated with respect to DCPD, octacalcium phosphate (OCP), and HAp, respectively [33, 34]. These facts support the proposed mechanism that CO_2 affect the self-setting process of TeCP-DCPD apatite cement.

Conclusions

The HAp formation process from DCPD and TeCP suspension has been investigated by ATR-IR and chemoinformatics. The differentiated score is useful for understanding the complicated chemical reactions involved. The proposed approach is found useful for analyzing the rapid reaction such as the self-setting TeCP-DCPD apatite formation of the present study. The setting formation of SSAC consists of three stages, and CO_2 plays an important role for the transformation as a catalyst. We are studying on the polymorphic transformation of carbamazepine by the proposed approach and getting informative results. The results will be published elsewhere in the near future.

Acknowledgments This research was partly supported by an Aspire Travel Grant from Tokushima University Foundation.

References

1. Brown WE, Chow, LC (1985) Dental restorative cement pastes, US Patent No. 4518430A
2. Denissen HW, de Groot K et al (1980) Tissue response to dense apatite implants in rats. *J Biomed Mater Res* 14(6):589–597. doi:10.1002/jbm.820140603
3. Hong YC, Wang JT et al (1991) The periapical tissue reactions to a calcium phosphate cement in the teeth of monkeys. *J Biomed Mater Res* 25(4):485–498. doi:10.1002/jbm.820250406
4. Constantz BR, Ison IC et al (1995) Skeletal repair by in situ formation of the mineral phase of bone. *Science* 267(5205):1796–1799. doi:10.1126/science.7892603
5. Hamanishi C, Kitamoto K et al (1996) A self-setting TTCP-DCPD apatite cement for release of vancomycin. *J Biomed Mater Res* 33(3):139–143. doi:10.1002(SICI)1097-4636(199623)
6. Hamada H, Ohshima H, Otsuka M (2012) Dissolution medium responsive sinvastatin release from biodegradable apatite cements and the therapeutic effect in osteoporosis rats. *J Appl Biomater Funct Mater* 10(1):22–28. doi:10.5301/JABFM.2012.9272
7. Miyamoto Y, Ishikawa K et al (1995) In vivo setting behavior of fast-setting calcium phosphate cement. *Biomaterials* 16(11):855–860. doi:10.1016/0142-9612(95)94147-D
8. Petrov I, Soptrajanov B (1967) Infra-red investigation of dicalcium phosphates. *Spectrochim Acta A Mol Spectrosc* 23(10):2636–2646. doi:10.1016/0584-8539(67)80155-7
9. Chang MC, Tanaka J (2002) FT-IR study for hydroxyapatite/col lagen nanocomposite site cross-linked by glutaraldehyde. *Biomaterials* 23(24):4811–4818. doi:10.1016/S0142-9612(02)00232-6
10. Ronson TK, McQuillan AJ (2002) Infrared spectroscopy study of calcium and phosphate ion coadsorption and of brushite crystallization on TiO_2 . *Langmuir* 18(12):5019–5022. doi:10.1021/la011676q
11. Ulian G, Valdre G, Corno M, Ugliengo P (2013) The vibrational features of hydroxylapatite and type A carbonated apatite: a first principle contribution. *Am Mineral* 98(4):752–759. doi:10.2138/am.2013.4315
12. Nres T, Isaksson T, Feam T, Davies T (2002) A user-friendly guide to multivariate calibration and classification. NTR publications, Chichester

13. Martens H, Nres T (1989) *Multivariate calibration*. Wiley, Chichester
14. Halaka FG, Babcock GT, Dye JL (1985) The use of principal component analysis to resolve the spectra and kinetics of cytochrome c oxidase reduction by 5,10-dihydro-5-methyl phenazine. *Biophys J* 8(2):209-219
15. Otsuka Y, Yamamoto M, Abe H, Otsuka M (2013) Effects of polymorphic transformation on pharmaceutical properties of direct compressed tablets containing theophylline anhydrate bulk powder under high humidity. *Colloids Surf B: Biointerfaces* 102:931-936
16. Otsuka Y, Yamamoto M, Tanaka H, Otsuka M Predictive evaluation of pharmaceutical properties of direct compression tablets containing theophylline anhydrate during storage at high humidity by near-infrared spectroscopy. *Bio-Med Mater Eng* in press
17. CAMO Software Research & Development Team "Welcome to the Unscrambler® X" <http://support.camo.com>
18. Shinzawa H, Awa K, Kanematsu W, Ozaki Y (2009) Multivariate data analysis for Raman spectroscopic imaging. *J Raman Spectrosc* 40(12):1720-1725. doi:10.1002/jrs.2525
19. Hayakawa S, Kanaya T et al (2013) Heterogeneous structure and in vitro degradation behavior of wet-chemically derived nanocrystalline silicon-containing hydroxyapatite particles. *Acta Biomater* 9(1):4856--4867. doi:10.1016/j.actbio.2012.08.024
20. Otsuka M, Matsuda Y et al (1995) Effect of particle size of metastable calcium phosphates on mechanical strength of a novel self-setting bioactive calcium phosphate cement. *J Biomed Mater Res* 29(1):25-32. doi:10.1002/jbm.820290105
21. Hsu J, Fox JL et al (1994) Metastable equilibrium solubility behavior of carbonated apatites. *J Colloid Interface Sci* 167(2):414-423. doi:10.1006/jcis.1994.1376
22. Rehman I, Bonefield W (1997) Characterization of hydroxyapatite and carbonated apatite by photo acoustic FTIR spectroscopy. *J Mater Med* 8(1):1-4. doi:10.1023/A:1018570213546
23. LeGeros RZ (1991) In: Myers HM (ed) *Calcium phosphates in oral biology and medicine*. Monographs in oral sciences. 15. Karger, Basel
24. Legeros RZ, Trautz OR, Legeros JP, Klein E, Shirra WP (1967) Apatite crystallites: effects of carbonate on morphology. *Science* 155(3768):1409-1411
25. Müller L, Conforte E, Caillard D, Frank, Müller A (2007) *Biomol Eng* 24(5):462-466. doi:10.1016/j.bioeng.2007.07.011
26. Otsuka M, Papangkorn K, Baig AA, Higuchi WI (2012) Chernometric evaluation of physicochemical properties of carbonated-apatitic preparations by Fourier transform infrared spectroscopy. *J Biomed Mater Res A* 100(8):2186-2193. doi:10.1002/jbm.a.33243
27. Elliott JC, Holcomb DW, Young RA (1985) Infrared determination of the degree of substitution of hydroxyl by carbonate ions in human dental enamel. *Calcif Tissue Int* 37(4):372-375. doi:10.1007/BF02553704
28. Otsuka M, Matsuda Y, Wang Z, Fox JL, Higuchi WI (1997) Effect of sodium bicarbonate amount on in vitro indomethacin release from self-setting carbonated-apatite cement. *Pharm Res* 14(4):444-449
29. Welch MJ, Lifton JF, Seck JA (1969) Tracer studies with radioactive oxygen-15. Exchange between carbon dioxide and water. *J Phys Chem* 73(10):3351-3356. doi:10.1021/j100844a033
30. Fukase Y, Eanes ED, Takagi S, Chow LC, Brown WE (1990) Setting reactions and compressive strength of calcium phosphate cements. *J Dent Res* 69:1852-1856
31. Otsuka M, Matsuda (1991) Effect of CO₂ laser irradiation on surface hardness of self-setting hydroxyapatite cement. *Chem Pharm Bull* 39(10):2753-2755
32. Doi Y, Shibata S, Takezawa Y, Wakamatsu N, Kamemizu H, Iijirna M, Moriwaki Y, Katsumi U, Kubo F, Haeuchi Y (1988) Self-setting apatite cement : III, setting mechanism. *Jpn Soc Dent Mater Devices* 7(2):176-183
33. Eidelman N, Chow LC, Brown WE (1987) Calcium phosphate saturation levels in ultrafiltered serum. *Calcif Tissue Int* 40(2):71-78
34. Eidelman N, Chow LC, Brown WE (1987) Calcium phosphate phase transformations in serum. *Calcif Tissue Int* 41(1):18-26. doi:10.1007/BF02555126